minerals

MDPI

Article

3D Geological Model of the Touro Cu Deposit, A World-Class Mafic-Siliciclastic VMS Deposit in the NW of the Iberian Peninsula

Mónica Arias [1], Pablo Nuñez [2], Daniel Arias [3], Pablo Gumiel [4], Cesar Castañón [5], Jorge Fuertes-Blanco [3] and Agustin Martin-Izard [3,*]

1 Consulting de Geología y Minería (CGM), S.L., C/Vista de la Ermita 1, 45930 Mentrida, Spain; monica.arias.llorente@gmail.com
2 Cobre San Rafael, S.L., Avenida de Santiago Nº42. 15823 O Pino, Spain; pablo.nunez@atalayamining.com
3 Department of Geology, University of Oviedo, C/Arias de Velasco s/n, 33005 Asturias, Spain; darias@geol.uniovi.es (D.A.); jorgefuert@gmail.com (J.F.-B.)
4 Department Geology, Ibercreta Group, University of Alcalá, 28805 Alcalá de Henares, Spain; pablo.gumiel@uah.es
5 Department of Mines Research, University of Oviedo, E-33004 Oviedo, Spain; castanoncesar@uniovi.es
* Correspondence: amizard@uniovi.es

Abstract: The Touro volcanogenic massive sulfide (VMS) deposit is located in the NW of the Iberian Variscan massif in the Galicia-Trás-os-Montes Zone, an amalgamation of several allochthonous terrains. The Órdenes complex is the most extensive of the allochthone complexes, and amphibolites and paragneisses host the deposit, characterized as being massive or semimassive (stringers) sulfides, mostly made up of pyrrhotite and chalcopyrite. The total resources are 103 Mt, containing 0.41% copper. A 3D model of the different orebodies and host rocks was generated using data from 1090 drill core logs. The model revealed that the structure of the area is a N–S-trending antiform. The orebodies crop out in the limbs and in the hinge zone. The mineralized structures are mostly tabular, up to 100 m in thickness and subhorizontal. Based on the petrography, geochemistry and the 3D model, the Touro deposit is classified as a VMS of the mafic-siliciclastic type formed in an Ordovician back-arc setting, which was buried and metamorphosed in Middle Devonian.

Keywords: 3D geological model; VMS; Galicia-Trás-os-Montes; Variscan Iberian Massif; Touro deposit

Citation: Arias, M.; Nuñez, P.; Arias, D.; Gumiel, P.; Castañón, C.; Fuertes-Blanco, J.; Martin-Izard, A. 3D Geological Model of the Touro Cu Deposit, A World-Class Mafic-Siliciclastic VMS Deposit in the NW of the Iberian Peninsula. *Minerals* **2021**, *11*, 85. https://doi.org/10.3390/min11010085

Received: 13 November 2020
Accepted: 13 January 2021
Published: 16 January 2021

1. Introduction

The Touro copper deposit is located in the NW of the Iberian Massif, which has been divided into four zones [1–3]. Three of these, the Central Iberian Zone, the allochthonous Galicia-Trás-os-Montes Zone (GTOMZ) lying above it, and the Astur-Occidental Leonesa zone, represent the internal zones of the Orogen, and the so-called Cantabrian zone forms the external zone (Figure 1A). The copper ores identified in the NW of the Iberian Massif are hosted by the so-called allochthonous complexes of the GTOMZ (Figure 1B) [1], which are emplaced over the Central Iberian Zone.

Numerous recent works dealing with the regional geology and the origin of the complexes have been published [4–9], but only a few papers refer to the geology and origin of these massive sulfides [10–13], whose geometry and relationships remain unknown. Badham and Williams [10] described the petrography and geochemistry of the Touro deposit and discussed its geological context. They suggested that Touro might be a metamorphosed Besshi-type ore (siliciclastic-mafic [14]). They finally attributed it to a Cyprus type (mafic [14]) metamorphosed ophiolitic VMS deposit of the Cu-Zn type. Moreover, Serranti et al. [12] indicate that the chemical composition of anomalous garnet-rich am-

phibolites (Ca-poor and Fe-rich) corresponds to products of polyphase metamorphism of hydrothermally altered mafic rocks and should be considered as a target for exploration.

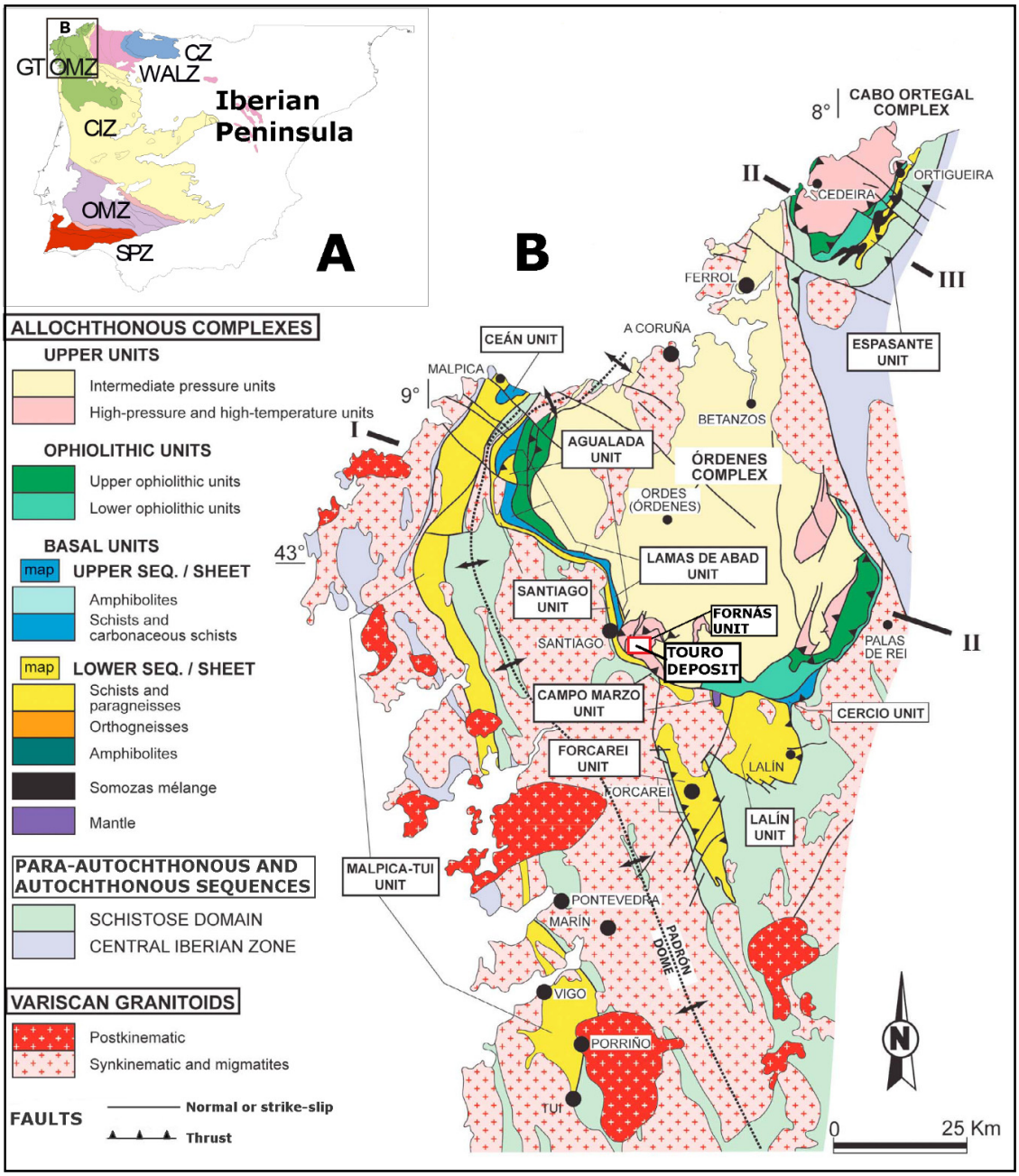

Figure 1. (**A**) Geological map of the Iberian Variscan Massif. CZ: Cantabrian Zone, WALZ: West Asturian Leonese Zone, CIZ: Central Iberian Zone, OMZ: Ossa Morena Zone, and SPZ: South Portuguese Zone. (**B**) Geological map of the NW Iberian Massif showing the location of the different allochthonous units of Galicia-Trás-Os-Montes Zone and the Central Iberian Zone. Adapted from [8].

In all these previous works on the deposits, the geometry and relationships between the different orebodies in the Touro ore remain undescribed. The present study deals with the petrographic characterization of the deposit and host rocks, which are in agreement with published works [10,13], a comparative geochemical study, and a 3D local, detailed modeling of an area of around 25 km^2, exclusively centered in the different sulfide masses of the Touro deposits and their host rocks (Figure 2). The 3D model highlights the geometry of the massive sulfides, host rocks, folds and their relationships.

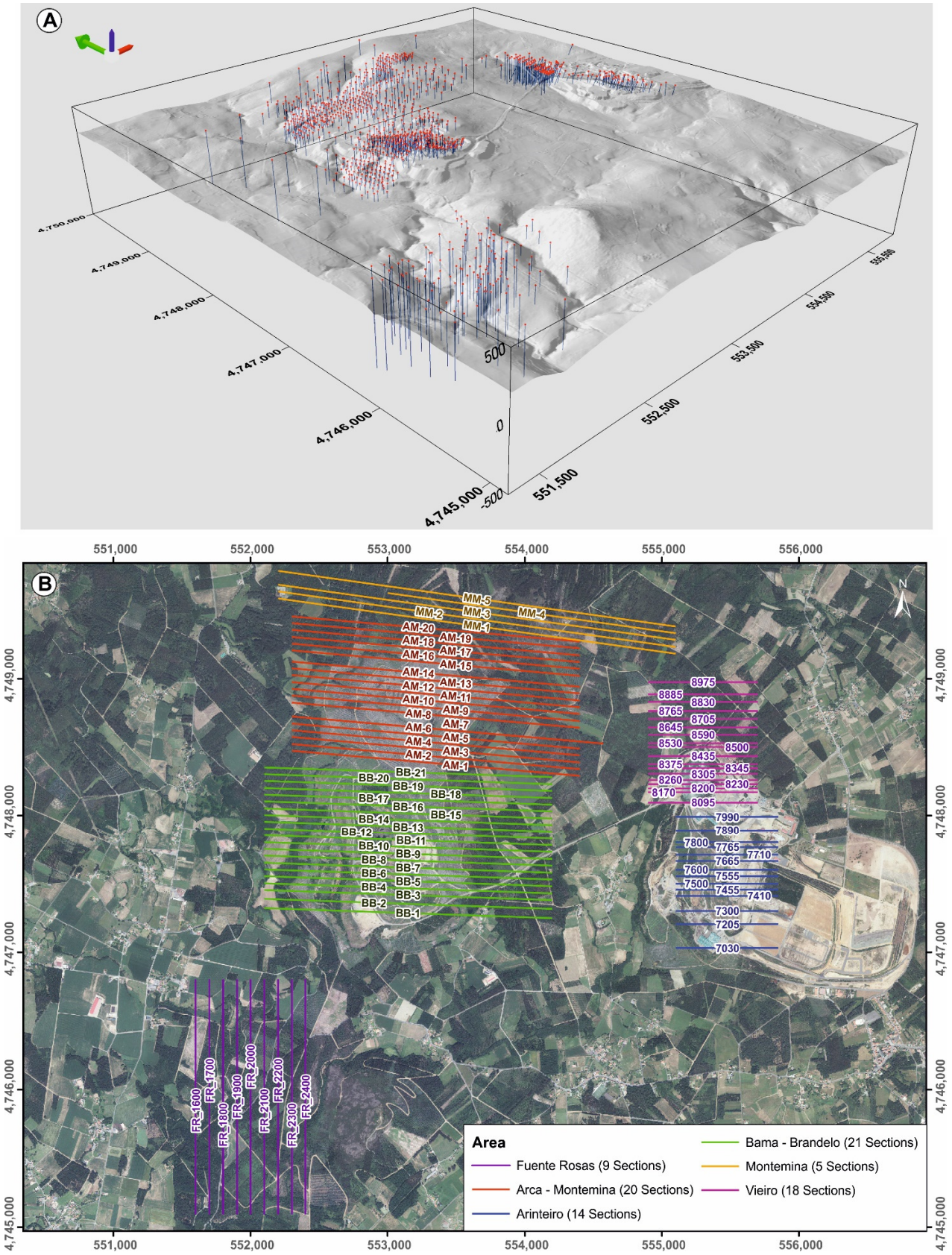

Figure 2. (**A**) Location of the 1090 utilized boreholes from different surveys with the digital elevation model (DEM) of the area. Information provided by Atalaya Mining. (**B**) Location of the 78 E–W and 9 N–S cross-sections generated, based on the thorough study and relogging of the drill cores used for building up the 3D model.

To reach this goal, we relogged 1090 boreholes (Figure 2A) in an attempt to unify the criteria used by different geologists in logging operations to enable us to establish a coherent geological database. This database allowed us to carry out a detailed model of the structure of the deposits through the generation of 87 cross-sections (Figure 2B) and also the subsequent 3D modeling technique presented for the first time in this work.

This 3D modeling technique proves to be very useful for solving many geological problems, as indicated by [15–17]. In these papers, the authors indicate that this 3D modeling technique, together with classical studies such as petrography or geochemistry, helps achieve a better understanding of the structural configuration of the deposits and provides guidelines for prospecting. It also helps improve the evaluation and exploitation of these VMS deposits.

2. Mineral Exploration and Mining

The Touro deposit is located 15 km to the east of Santiago de Compostela in the Fornás unit (Figure 1B). The deposit outcrops along an antiform measuring around 5 km from east to west and about 5 km from north to south.

The history of mineral exploration and mining in the Touro area started in the copper age, between the 10th century BC and 1st century AD [18], a period in which small works were later recognized. Between the 17th and 19th centuries, prospecting activity around Santiago de Compostela increased, particularly in the Fornas ore body, and in 1835, Guillermo Schulz identified the presence of sulfides in the area. In 1903, The Coruña Copper Company Limited commenced an exploration program and described the ore, indicating a copper grade between 2% and 3% and estimated reserves of around 250 million tons that could be extracted by open-pit mining [19]. The funds available to the company were frequently used for opening trenches that did not produce the expected results. Due to this activity, today, we can find several small trenches and galleries in the north of the deposit and the area is now known as Monte das Minas (mine hill). All this activity was abandoned at the beginning of the First World War. After the end of the Second World War, exploration activity started again, and during the 1950s and 1960s, Touro and Pino were considered the most interesting areas.

At the end of the 1970s, the authors of [10] indicated the presence of four deposits, of which the Rio Tinto Patiño mining company was exploiting three: Fornás, Bama and Arinteiro. The first is located on the western side of the antiform and was on the point of being closed at that time after the extraction of 1.0 Mt with Cu grades between 1 and 2%. The fourth deposit, Monte das Minas, was abandoned in 1939, and there are no data referring to it. At that time, the authors of [10] indicated that Arinteiro had 12 Mt at 0.7% Cu and Bama had 20 Mt at 0.5% Cu. Rio Tinto Patiño never exploited the central part of the anticline where the old prospects known as Arca and Monte das Minas are located. The geological exploration in the area from 1960 to 1986 used 798 drill holes obtaining 106,000 m of drill cores. In 1973, Rio Tinto Patiño, S.A commenced exploitation, extracting around 1.5 Mt per year until 1986, the year in which the mining company stopped production due to the low price of copper. The historical production was 800,000 tons of copper concentrate (190,000 tons of Cu metal, 1 million ounces of silver and 70,000 ounces of gold). During 2012, Lundin Mining made 169 drill holes, obtaining over 20,000 m of drill cores and over 7600 analyzed samples. Since 2015, Atalaya Mining has performed 423 drill cores, with a total of 45,000 m and analyzed 20,400 samples. All these data have permitted Atalaya [20] to define a resource of 103 Mt with an average Cu of 0.41%, Touro being one of the biggest copper deposits in Europe and a world-class type.

3. Geological Setting

The Iberian Massif represents one of the best sections of the Variscan Orogeny, developed between the Devonian and Permian (400–290 million years). The Orogeny occurred during the collision between Gondwana and Laurussia, giving way to the Pangea supercontinent [21,22].

The NW of the Iberian Massif represents the European Variscan suture, having remnants of fragments with both continental and oceanic affinities that show clear structural interrelationships. The Iberian Massif is characterized by its arcuate geometry, with its core in the region of Asturias (Asturian arc) due to the development of a secondary type oroclinal [7,8] during the last stages of the Variscan Orogeny (Moscoviense to Asseliense, ca. 310–297 Ma) that affected all the previous structures [23]. This secondary oroclinal geometry was developed during the collision between Laurussia to the north and Gondwana to the south [24,25]. The amalgamation of both continents gave way to the Pangea supercontinent after the Rheic Ocean closure at the end of the Carboniferous beginning of the Permian. This closure involved many other minor structures such as back-arc or pull-apart basins [26–32].

During the development of all these geological processes, the NW of the Iberian Peninsula was made up of an amalgamation of different terrains, including an autochthone and several allochthones. The exotic sheets preserved in the core of Late Variscan synclines make up the Galicia-Trás-os-Montes allochthones. In the Galicia region, there are three allochthone complexes: the Cabo Ortegal, Órdenes and, further west, the Malpica-Tuy unit, which is different from the other two (Figure 1B). The Órdenes complex is the biggest of the allochthonous complexes, being approximately 135 km × 75 km in size and having a rounded geometry due to its synform shape [33,34].

The copper ores identified in the NW of the Iberian Massif are hosted by the allochthonous complexes [1] emplaced over the Central Iberian Zone. The Galicia-Trás-os-Montes Zone allochthonous terrains have been subjected to a variety of tectonometamorphic conditions. Within this zone, fragments from a passive continental margin, areas that underwent rifting processes, remains of a volcanic arc and back-arc basins and several ophiolite units can all be distinguished. All these geological sheets preserved characteristics related to their relative original positions, lithology and tectonothermal evolution. This allowed them to be grouped into three units. From the bottom to the top, these units are basal, ophiolitic and upper. The upper unit, where the deposits are located, is also divided into two members: the high-pressure and temperature (HP-HT) unit at the bottom and the medium-pressure (MP) unit at the top. Both the basal and upper units of the Galicia-Trás-os-Montes Zone have a continental crust lithologic composition, including an island arc and back-arc basins. By contrast, the ophiolitic units derive from an oceanic crust (Figure 1B). All these units are separated by tectonic detachments, which from top to bottom are the so-called Corredoiras, Fornás and Bembibre-Ceán [6].

There are numerous copper deposits and prospects in the allochthonous complexes, mainly associated with the HP-HT units, but on some occasions, small bodies are related to the ophiolite units, as is the case of Moeche in the Cabo Ortegal Unit [35]. The geodynamic context for the magmatic (tholeiitic/kalcalkaline) rock formation of the HP-HT units is a volcanic magmatic arc and back-arc extensional basin [5,36–39].

During the accretion process and thrust, several deformational processes were registered. It is estimated that the main metamorphic event (HP-HT) was related to the first subduction event [40] associated with the beginning of the Variscan deformation (D1). The second event (D2) was related to decompression and partial melting of paragneisses and mafic lithologies [41]. Later on, D3 developed, with related folds and thrusts verging to the east [42].

The Touro deposit and other mineralized areas in the vicinity are located in the HP-HT lower member of the upper units. This unit has been described in five localities: Sobrado; Melide and Belmil in the southeast of the Órdenes Complex and Arinteiro; and Fornás [33,43] in the south, the latest hosting the Touro deposit. Badham and William [10] discussed how the geological context for the Touro deposit may be a metamorphosed Besshi type ore (siliciclastic-mafic [14]) but [10] proposed for Touro a Cyprus type (mafic [14]) metamorphosed ophiolitic VMS deposit of the Cu-Zn type.

The protolithologies for the two upper units (HP-HT and MP) are considered to be equivalent, but the intensity of metamorphism and deformation prevents us from recogniz-

ing the original sedimentary and igneous characteristics [6]. The most abundant lithologies are paragneisses and meta-mafic-ultramafic rocks such as garnet and clinopyroxene granulites and eclogites or their retrograde metamorphic equivalents such as amphibolites and greenschist [44–46]. The Fornás unit, where the Touro deposit is located, is characterized by the abundance of amphibolites hosted by the paragneisses. The most frequent are garnet amphibolites, with relicts of granulite minerals (Cpx-Grt-Pl. [6]) and metagabbros, all having different retrogradation from nearly untransformed to coronitic metagrabbro and granulites [43]. Within the gabbros, there are bodies of metaperidotites and pyroxenites up to 2 km in length. The chemical composition of gabbros is tholeiitic with MORB characteristics [44]. The upper medium-pressure unit of greywackes is separated from the HP-HT unit by the detachment of Corredoiras [39,47].

4. Materials and Methods

4.1. Mineralogy and Geochemistry

The realization of this study was possible because we had access to over 1400 drill-core logs from the Touro area (Figure 2A), from which we selected 1090. We revisited the drill cores made up by different mining companies in order to unify the logging criteria used and to take a detailed sampling of the ore-bearing rocks and host rocks of this deposit. Selected samples were chosen to perform polish-thin sections for mineralogical and petrographical studies and for mineral geochemistry. Twenty-five were studied using transmitted- and/or reflected-light microscopy, SEM-EDS and EPM (Cameca SX100 incorporating secondary electrons, backscattered electrons, absorbed detectors and energy-dispersive spectrometry) at Oviedo University (Oviedo, Spain). The analytical conditions and standards used are described in [48].

The geochemical rock data (mineralized and barren) came from the analysis performed by the mining companies (Lundin and Atalaya) at ALS Limited (Vancouver, Canada, Accredited Laboratory No. 579) using the Ultra-Trace Level Method ME-MS61. The method used combines four-acid digestion with ICP–MS instrumentation. The final solution is then analyzed by means of inductively coupled plasma–atomic emission spectrometry and inductively coupled plasma–mass spectrometry. Results are corrected for spectral interelement interferences. Of these analyses, we used 270 Fe, Ti, Al and Mn data from the Arca deposit.

The total resources estimated by the company are 103 Mt, having an average copper content of 0.41% [20]. For this estimation, they used the 3D geostatistical model called the "empty block model" created with cell dimensions of 10 m$\times$ 10 m $\times$ 10 m and comprising the whole amphibolite body and massive sulfides, but no 3D geological model was used. The evaluation method, uncertainties and results are available on the web at [20].

4.2. The Generation of the Touro 3D Geological Model

The use of 3D geological models to facilitate the understanding of surface and subsurface geology is well-established by many authors (i.e., [15–17,49–54]).

The methodology used in the Touro 3D geological modeling was implemented in a system consisting of a GIS, a spatial database and a 3D modeling software [53–56]. It involves several different steps for processing data, depending on the ore type (Figure 3A–C):

First step. Realization of the digital elevation model (DEM) using the ArcGIS 10.2© software (version 10.2, Esri©, Redlands, CA, USA) to model the topographic surface. Acquiring, compiling and standardizing the geological information and borehole data using Geosoft Target (version 4.4, Seequent Limited for Europe, Marlow, UK) for ArcGIS©. The sources of the datasets are:

A. Different drilling surveys performed from 1960 to that most recently carried out by Atalaya Mining were used to reconstruct the 3D geometry of the deposits. This involved access to over 1400 drill-core logs from the Touro area (Figure 2A), from which we selected 1090, containing valuable lithological or structural information and relogged these drill holes in an attempt to unify the criteria used by different geologists in logging operations. We grouped all the different kinds of rock into four lithologies: the paragneisses, the amphibolites, the massive sulfides, and the stringer zones. We considered rock as ore if its Cu content is over 0.2%. In fact, mineralization is much more broadly extended, but we set this limit based on the evaluation criteria used by Atalaya Mining Company [20]. All borehole data (coordinates, descriptions, depth, etc.) were stored in a database in which every hole had a unique identifier.
B. Topography at a 1:5000 scale from a topographical survey provided by the company.
C. Geological surface data from the authors.
D. Historical geological information on the surrounding mining areas and selection of usable data.

Second step. Hand drawing of 87 vertical cross-sections (78 E–W and 9 N–S) using the borehole data projected (10 m distance) on the sections (Figure 2B). Based on these, 2 horizontal sections, both at a 1:4000 scale, were generated. This methodology allowed us to produce a detailed construction of the structure of the deposit and is well known in geology, often being applied to mineral exploration and mining (i.e., [57,58]).

The vertical and horizontal sections were georeferenced and digitalized to produce the XYZ coordinates of each contact between the units and mineralized bodies defined in Step 1 and in the geological structures. All this digitized information, together with precise data such as dip and strike, was stored in a spatial database created in ArcGis 10.2©. In this step, the use of an advanced GIS allowed us to check the topology rules in order to ensure geometrical consistency.

During Steps 1 and 2, a validation process was performed with a view to keep accurate and reliable data and reject imprecise or uncertain data from the dataset before modeling.

Third step. All geological data, cross-sections, borehole data and DEM were imported from the database to GeoModeller©. Geological surface models were built by means of contact and dip vectors derived from the sections and DEM. The large number of drill hole data allowed us to validate the geological subsurface objects because they were used as a depth constraint.

Three-dimensional (3D) geological modeling was generated using GeoModeller© (www.intrepid-geophysics.com), original software developed at the BRGM (French Geological Survey; [59,60]). In this software, lithological units are described as a pseudostratigraphic pile, intended to image the geology and structural relationships as well as possible. A major feature of this tool is that the 3D description of the geological space is achieved through a scalar potential field formulation interpolated by universal cokriging [55]. The geological contacts are isopotential surfaces, and their dips are represented by gradients of the potential, being isolines in 2D or isosurfaces in 3D [61,62]. Taking into account both contact locations and orientation data, the 3D models were constructed using an implicit scalar method.

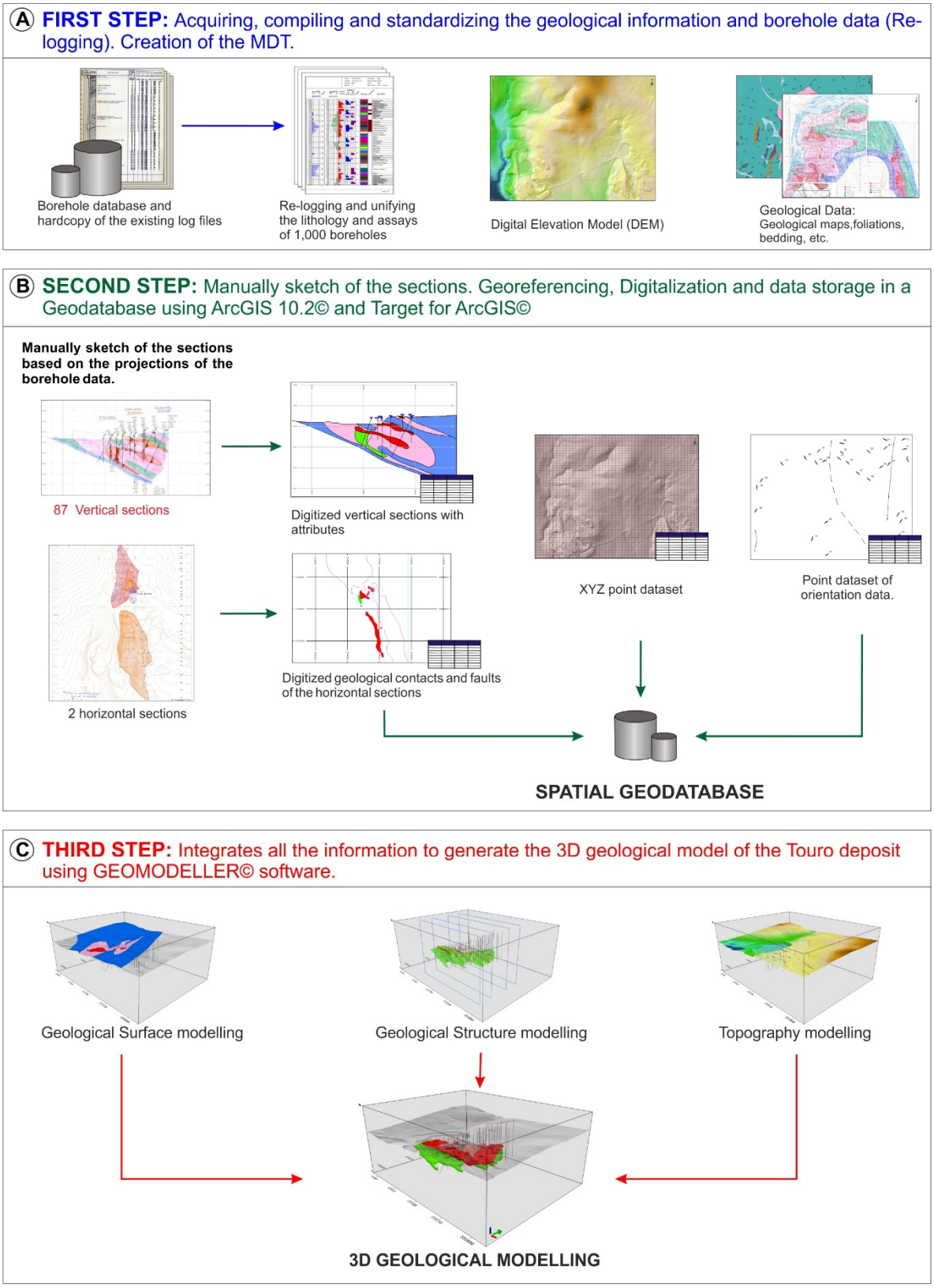

Figure 3. Chart of the applied methodology for 3D model generation. (**A**)First Step; (**B**) Second Step; (**C**) Third Step.

5. Geology of the Touro Cu Deposit

The rocks bearing the copper ore are located in the Arinteiro antiform formed during the last Variscan deformation stage. The geological maps and cross-sections performed in our work indicate that the massive sulfides at Touro are located in metamorphosed basalts hosted by a thick siliciclastic sequence metamorphosed to paragneisses.

A detailed microscope study allowed us to differentiate between three types of amphibolite, namely fine-grained dark-green amphibolite, garnet-rich porphyritic amphibolite and fine-grained pale-green garnet amphibolite. The first is a banded amphibolite made up of hornblende and plagioclase with minor amounts of chlorite, epidote and pyroxene. Its texture is ophitic defined by hornblende crystals. Castiñeiras [4] indicates the presence of relict textures of a gabbro rock. The amphibolite appears in contact with the paragneisses both at the top and at the bottom of the bodies. The garnet-rich porphyritic amphibolite is, in most cases, surrounded by the fine-grained dark-green amphibolite. The texture is porphyritic to nematoblastic, being Ca-poor. It is composed of chlorite, quartz and almandine garnet up to 3 cm in diameter and minor amounts of hornblende, plagioclase, actinolite, rutile and epidote-zoisite. The garnet constitutes about 25–35% of the rock. It has abundant opaque minerals, mostly pyrrhotite, chalcopyrite, sphalerite and pyrite. Carbonate is present as a secondary mineral. Between these two amphibolite types, there is a third type of transition amphibolite. It is a fine-grained schistose amphibolite, rich in chlorite and contains some garnets and titanite. It is poor in Ca and pale-green in color.

The paragneisses grain size is fine to medium, dark in color, has a lepidoblastic texture and is made up of plagioclase, quartz, muscovite, biotite, staurolite, sillimanite, kyanite, rutile, ilmenite, garnets, graphite and scarce sulfides (pyrrhotite and pyrite). The paragneisses are banded, having plagioclase and quartz-rich levels alternating with other mica-rich levels where graphite and sulfides are found.

The mineralized bodies (massive sulfides and stringers) outcrop along about 6 km both in the limbs and in the hinge zone of the Arinteiro N–S-trending antiform. The mineralized structures are mostly tabular, up to 100 m in thickness, subhorizontal and having quite a well-defined contact with the host rock. The Touro deposit has been divided into seven main ore bodies, Arinteiro, Vieiro, Arca, Monte Mina, Bama, Brandelos and Fuente Rosas and other minor ore bodies. In all the ore bodies, the mineralized mass is mainly hosted by garnet amphibolites, but at Arca and Monte das Minas, there are also mineralized bodies in the paragneisses below the amphibolites. This mineralization is characterized as being massive (with only some nonsulfide minerals disseminated in the rock) or semimassive sulfides, in the latter case having a breccia texture with fragments of rock made up of plagioclase, phlogopite, hornblende, clinozoisite, epidote and quartz cemented by pyrrhotite-chalcopyrite (Figure 4). The rock fragments were designated "rolled-balls" by [10]. The richest Zn zones (up to 0.47%) are related to this mineralization, and no lead minerals were detected.

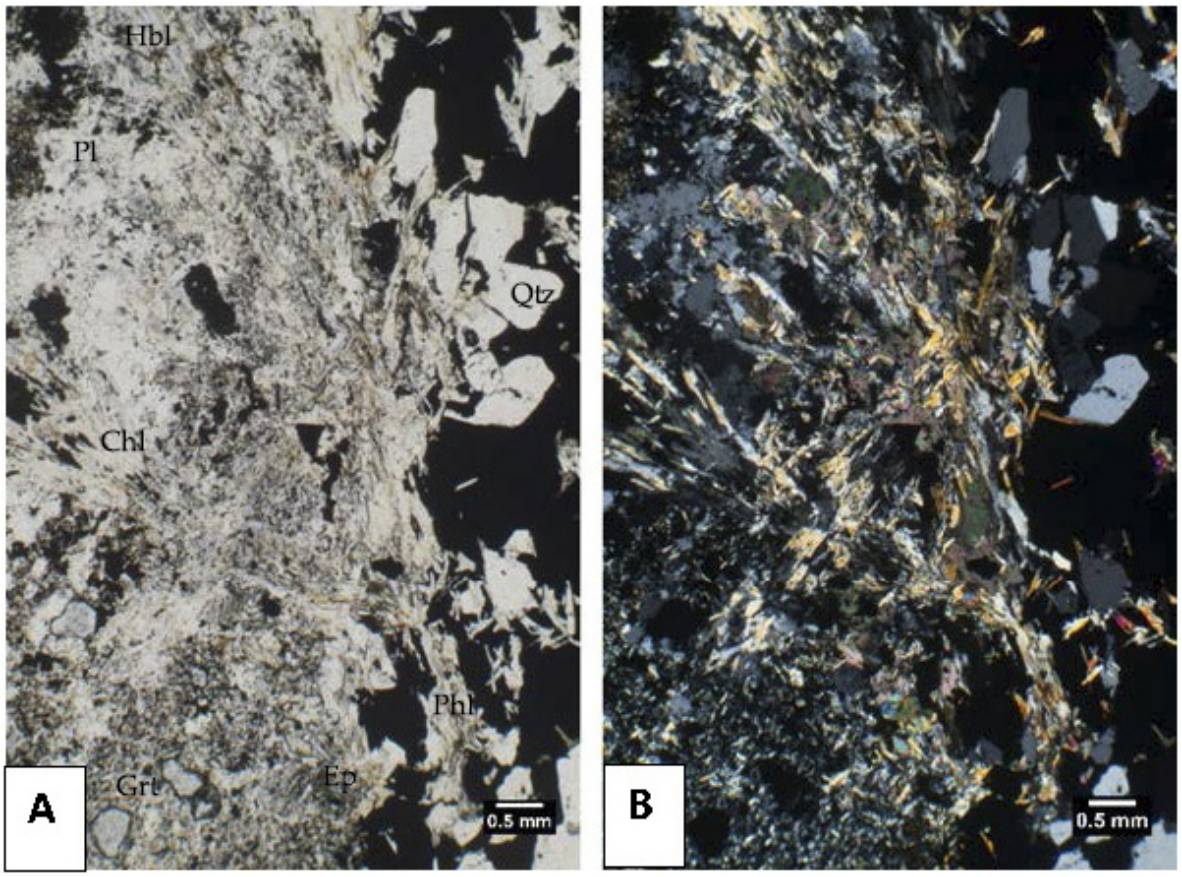

Figure 4. Microscopic view of thin section IAC-49C under plane-polarized light (**A**) and the same mineral assemblage, under cross-polarized light (**B**), of the stringer zones ("rolled-balls") of the Touro deposit. The left side of the section corresponds to a rock made up mainly of plagioclase, phlogopite, chlorite, hornblende, garnet and epidote-clinozoisite crosscut by a vein (right side) composed of quartz, opaque minerals and some phlogopite.

The strong deformation and metamorphism and the later retrograde metamorphism prevent us from using the Touro drill cores and thin sections for the purpose of recognizing the stringer zones of the mineralized areas. Nevertheless, in some of these areas, a brecciated stringer zone is detected (mineralized brecciated garnet amphibolites having an angle to the rest of the sulfides and showing two preferential directions, N–S-trending (Vieiro) and E–W-trending (Fuente Rosas). More breccia zones are found in other masses, but the relationships between the different bodies are not possible to determine accurately due to the strong deformation and the presence of possible folded zones during the D1 deformation stage. All the rocks are foliated, giving rise to S-type mylonites. The general trend of the foliation is N–S dipping 30°–40° to the west. The copper ore is located in the stringer, and at the bottom of the basalt laccolith, the stringer zone gives way to deformed stockworks (breccias) and replacements of the basalts and, on some occasions, the paragneisses. The metallic mineral paragenesis is mostly composed of pyrrhotite and chalcopyrite with minor amounts of pyrite and sphalerite. The richest zones in Cu are located at the contact between the stockwork and the replaced basalt. The copper-rich body (>0.2% Cu) is surrounded by a pyrrhotite mass.

As mentioned, the mineralized bodies are hosted in a garnet-rich amphibolite, which is included in a fine-grained amphibolite. Some preliminary geochemical data from both the amphibolites and paragneisses are given in Figure 5. We took as a reference the Arca ore body because, in it, the mineralized paragneisses are abundant and representative while, in other ore bodies, they are scarcer and not well represented, but the results in all the deposits are quite similar.

We plotted some geochemical results in Figure 5, the diagram proposed by [63] and modified by [64,65]. In accordance with these data, most of the paragneisses plot in a cluster over the Pacific Ocean pelagic sediments and terrigenous sediments plot. In addition, most of the amphibolites plot in a cluster at the average MORB value. By contrast, both mineralized garnet amphibolite and mineralized paragneisses show a tendency of amphibolites and paragneisses to mix with metalliferous sediments of the Red Sea and East Pacific rise.

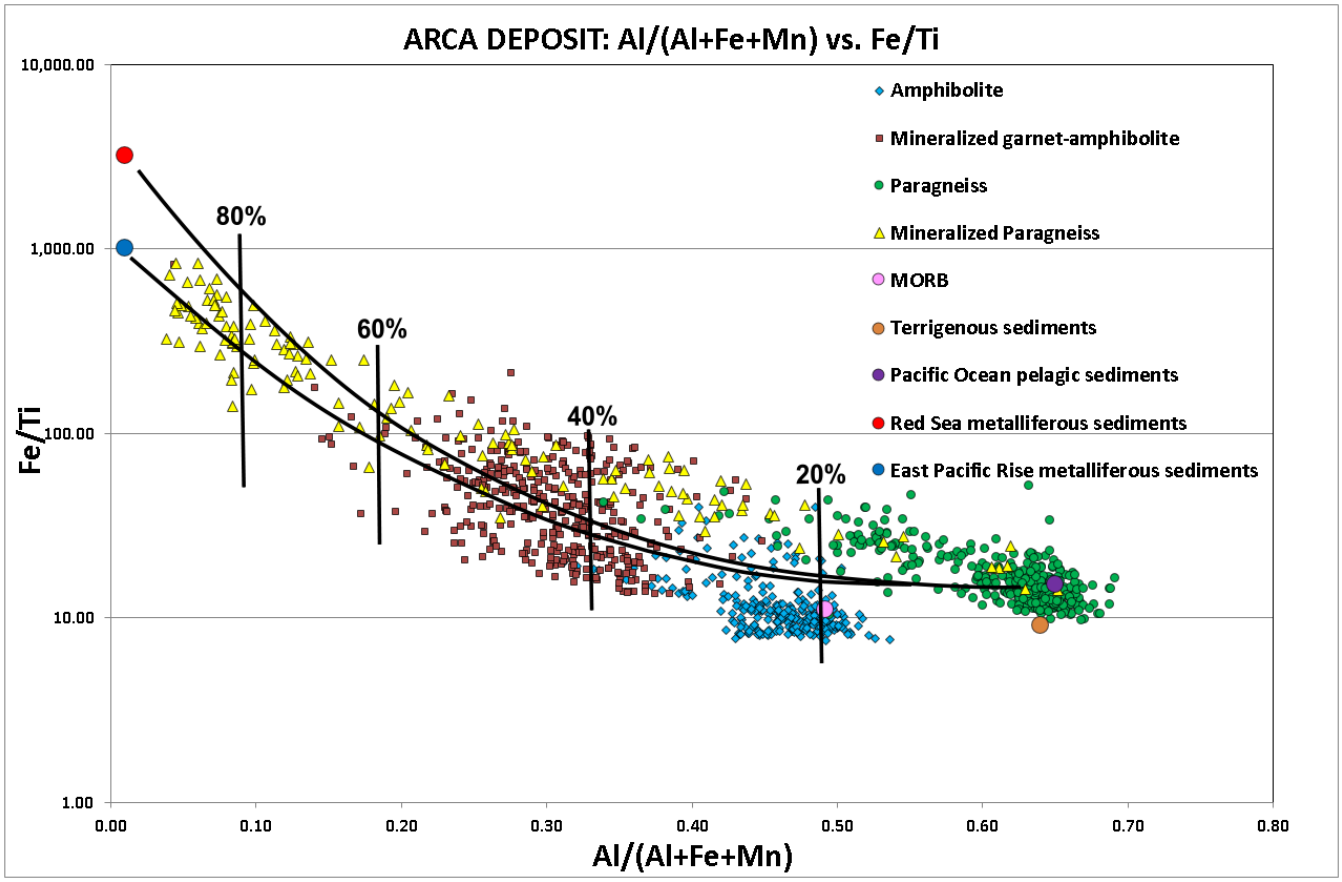

Figure 5. Fe/Ti vs. Al/(Al + Fe + Mn) plot from the Arca deposit. Shown also for reference are average compositions for metalliferous sediments from the Red Sea, the East Pacific Rise, pelagic sediment from the Pacific Ocean, terrigenous sediments [64] and average value of MORB.

6. Results and Structural Characteristics of the Touro 3D Geological Model

An important contribution of this 3D geological model to the knowledge of the structural evolution of the area is the modeling of a roughly N–S-trending antiform, the Arinteiro antiform. This fold shows a subvertical axial plane, with the fold axis plunging toward the north (Figure 6 and Figure S1). The ore bodies (massive sulfides) outcrop over approximately 8 km both on the limbs and in the hinge zone of the antiform (Figure 6 and Figure S1). The massive sulfides are located in the western limb (Arca, Bama, Brandelo and Fuente Rosas) and the eastern limb (Vieiro and Arinteiro) of the fold and in the hinge zone (Monte Mina) (Figure 6). The mineralized structures are mostly tabular, up to 100 m in thickness, subhorizontal and have a well-defined contact with the host rocks (Figure 7A,B). The Arinteiro and Viero massive sulfides, in the eastern limb, dip at around 25–30° to the east (Figure 7B and Figure 9). The Fuente Rosas massive sulfides, in the western limb, dip around 35° to the west (Figure 8 and Figure 10).

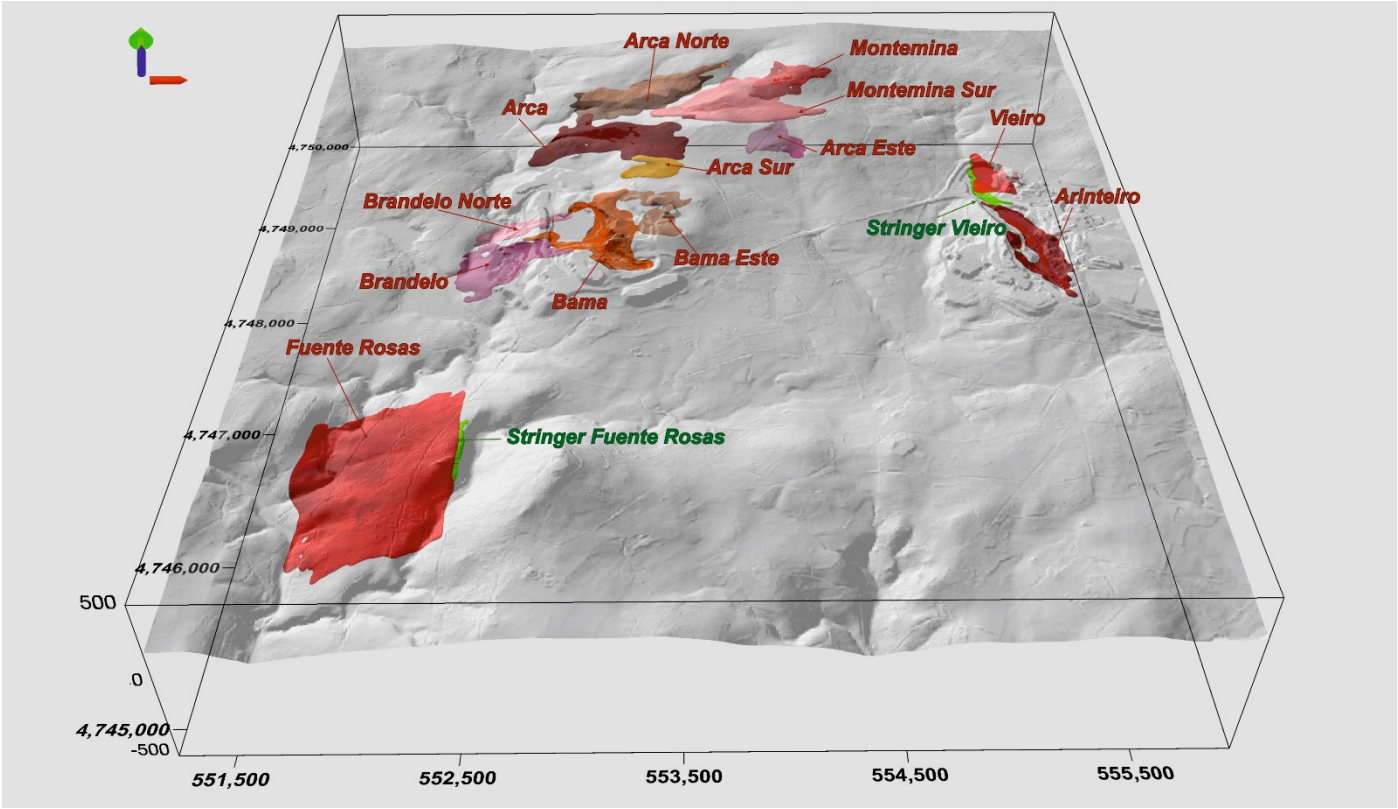

Figure 6. General view, from the south, of the whole modeled area showing the different lenses of massive sulfides in the western and eastern limbs and in the hinge zone of the antiform. The stringer zones of Fuente Rosas and Vieiro (light green) are also labeled.

The host rocks of the deposits are mainly amphibolites showing lenticular morphology (Figure 7A,B and Figure 8; Figures S2 and S3). Both the strong deformation and metamorphism make it difficult to recognize the stringer zones of the mineralized areas, but in some areas, a brecciated stringer zone showing two preferential directions is detected: N–S-trending (Vieiro, Figures 7B and 9) in the eastern limb and E–W-trending (Fuente Rosas) in the western limb (Figures 7A, 8 and 10). Both are probably related to the old Ordovician fracture system formed during a rifting process. These stringer zones are located below the massive sulfides and at a low angle to them (Figures 7, 9 and 10).

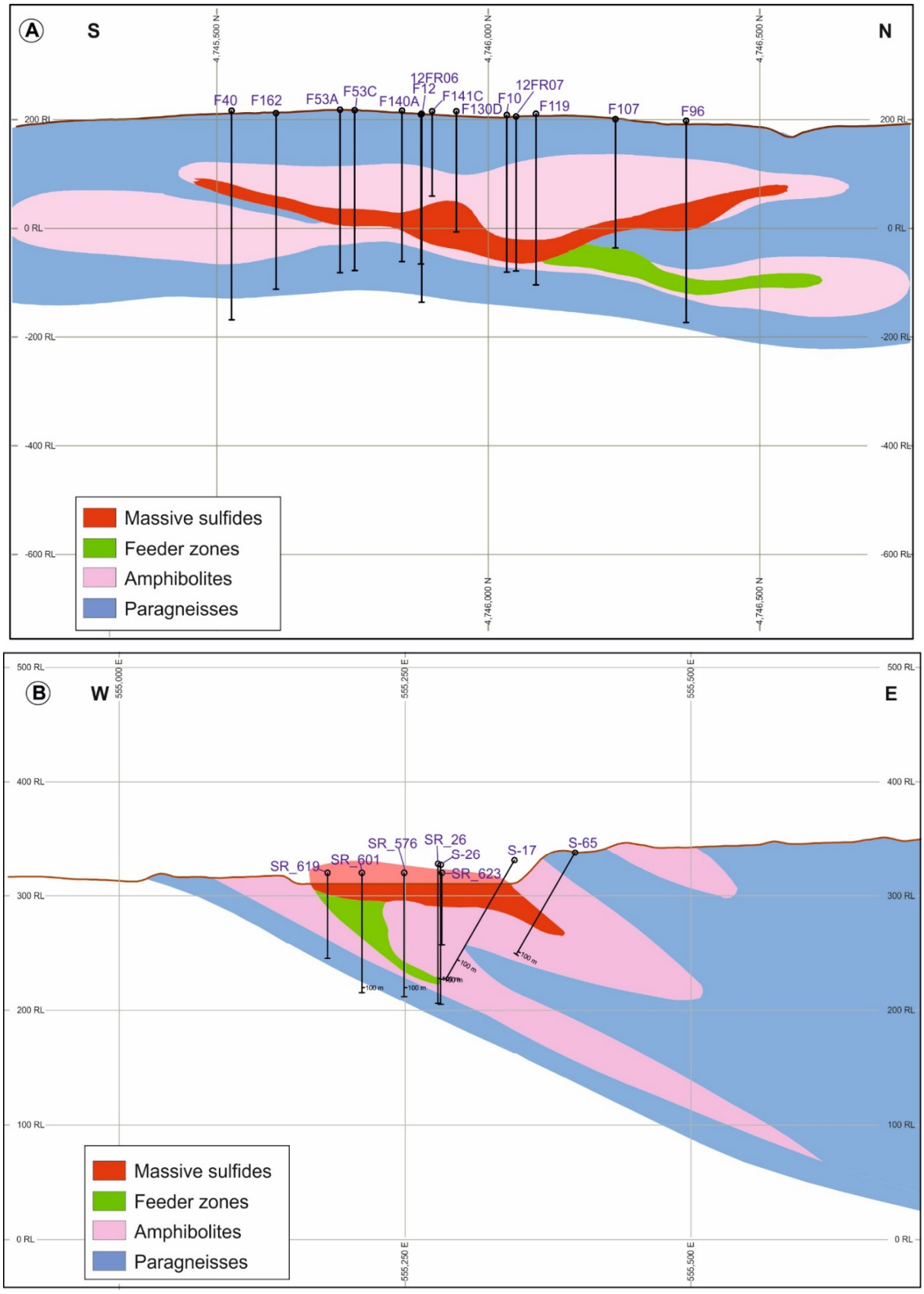

Figure 7. Two representative geological sections of the Touro deposit: (**A**) Section 2000 in Fuente Rosas and (**B**) Section 8200 in Vieiro. Both sections were selected from 87 sections generated from drilling data. For an explanation, see text.

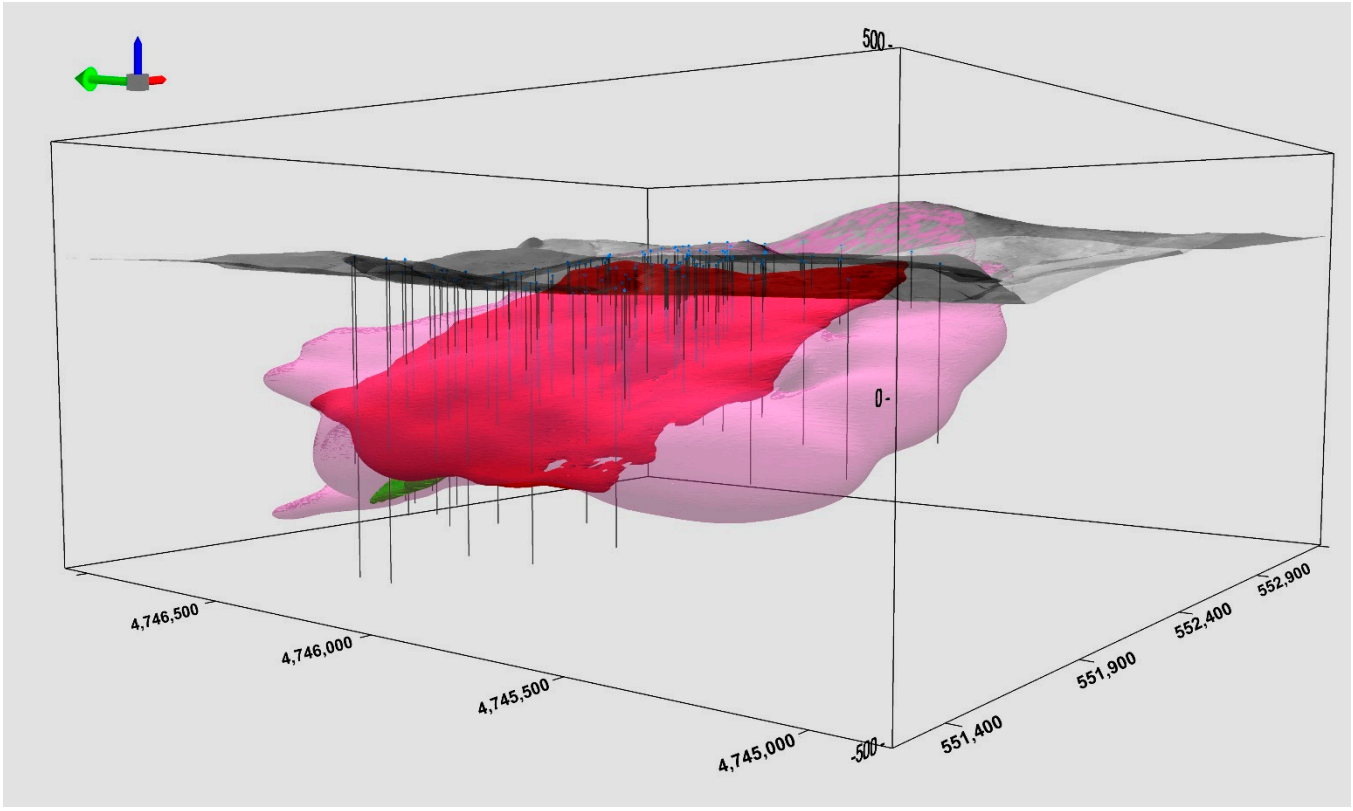

Figure 8. A 3D view, from the southwest, of the Fuente Rosas modeled area. The amphibolites are represented in pink, the massive sulfides in red and the stringer zone, which is mainly included in the amphibolites, in green.

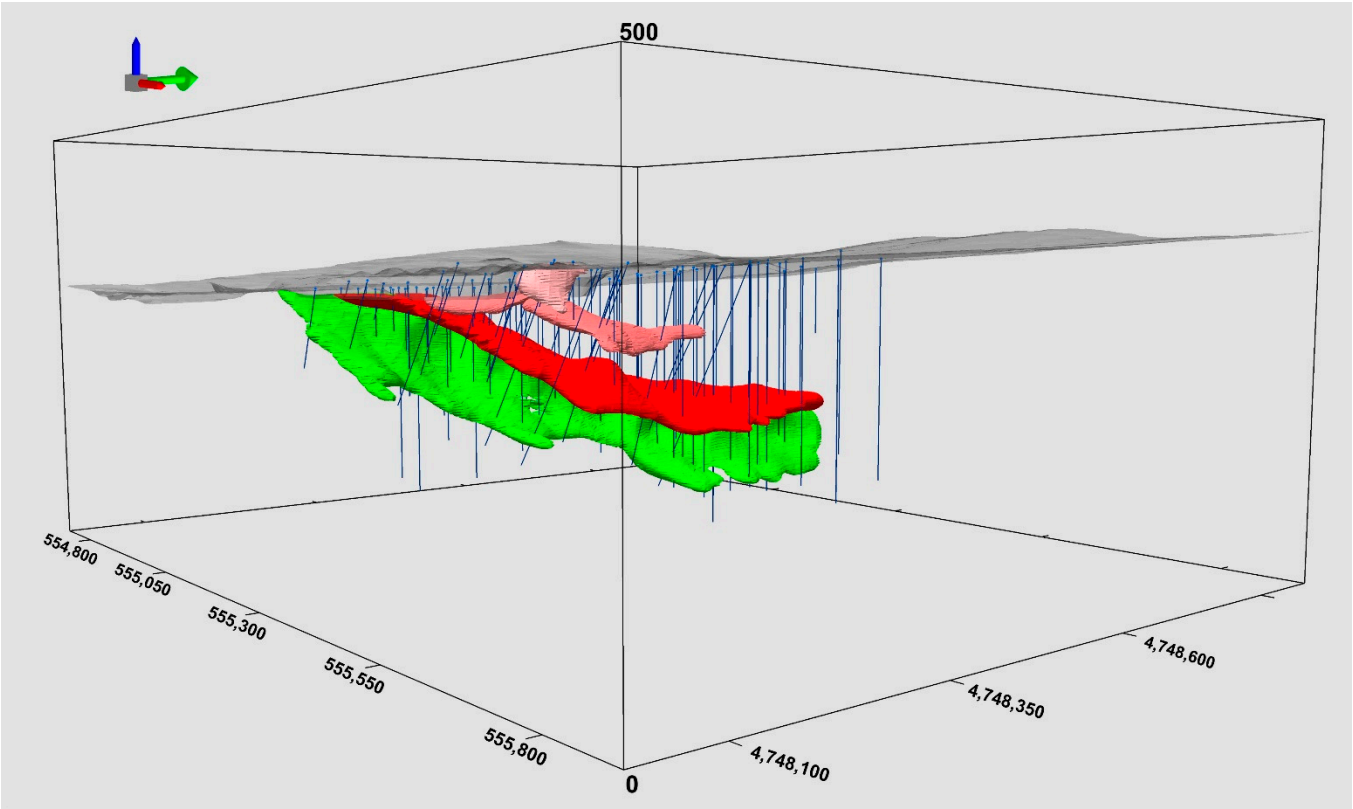

Figure 9. A perspective from the southeast of the Vieiro modeled area. The massive sulfides (in red) gently dip around 25–30° to the east, and the stringer zone (in green) is located below the massive sulfides at a low angle to them. The drill traces are included.

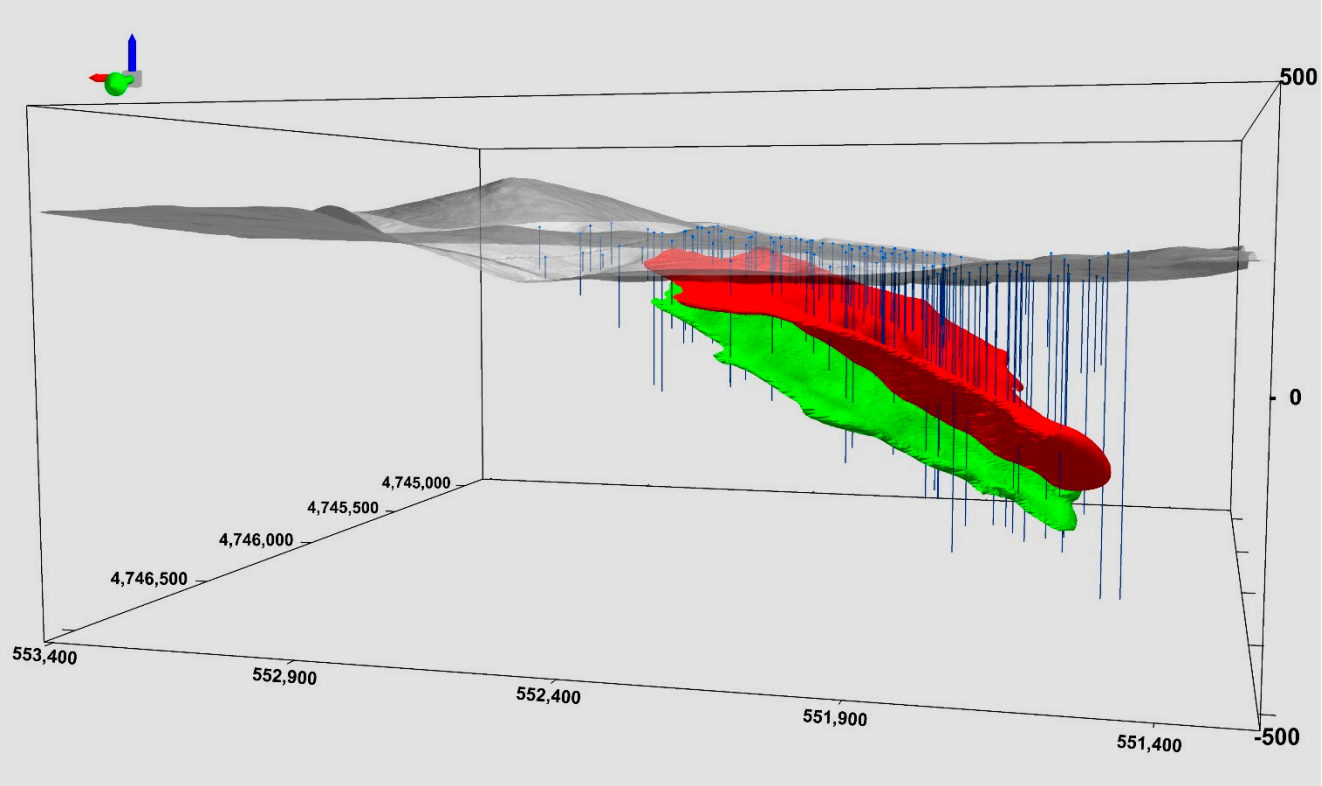

Figure 10. A perspective from the north of the Fuente Rosas modeled area. The massive sulfides (in red) dip around 35° to the west, and the stringer zone (in green) is also represented.

7. Discussion

The general structure of Touro resulted from three main periods of formation (Table 1). The first, during Ordovician times (±480 Ma), must have been largely transtensional, with the depositing of siliciclastic sediments in a back-arc extensional basin setting, including basaltic volcanism and the formation of the Volcanic Massive Sulfide deposits. Many authors [4–10,12,13,41–50] describe the general characteristics of this geological setting. The VMS bodies are mostly hosted in the basalts but quite frequently also in the siliciclastic sediments, as can be seen in the sections and in the 3D model (Figures 7 and 8). The breccia ores are interpreted in this work as feeder zones, which are probably related to the old Ordovician fracture system formed during a rifting process. The hydrothermal fluids from which the ore was precipitated may well have metasomatized both the basalts and the siliciclastic sediments, leading to the possible formation of abundant chlorite, among other minerals. As stated in Figure 3 and in the 3D views (Figures 6–10), the conditions for the VMS formation appear to have taken place in this type of geodynamic setting.

After the formation of the deposit in Ordovician times, the second step was the burial of the siliciclastic sediments, mafic rocks and VMS at depths of around 10 km. These rocks were metamorphosed under amphibolite facies, the siliciclastic rocks becoming parag-neisses, sometimes with high graphite contents (black shales or carbonates), and the basaltic rocks were transformed into amphibolites during Early Devonian (410–390 Ma [66–69]) and the hydrothermally affected host rocks into iron-rich, calcium-poor and chlorite-rich garnet amphibolite and gneisses. Thus, the anomalous Ca-poor amphibolites are interpreted as metamorphosed basalts, hydrothermally altered and metasomatized, and mineralized paragneisses are the metamorphic result of metasomatized and mineralized siliciclastic sediments.

Table 1. Summary of the three main periods of Touro deposit formation.

Periods of Formation	Tectonic Setting	Processes Involved	Ore and Rocks	Structural Elements
First step: Early Ordovician (±480 Ma)	Extensional back-arc basin setting (transtension)	Deposition of siliciclastic sediments. mafic rocks emplacement as sills	Formation of VMS deposits. Host rock is hydrothermally affected	Normal extensional faults
Second step: Early Devonian (410–390 Ma)	Burial of siliciclastic sediments, mafic rocks and VMS	Metamorphism of siliciclastic sediments, mafic rocks and VMS under amphibolite facies	Transformation of rocks into amphibolites and paragneisses	Foliation in all the rocks. development of S-type mylonite folds
Third step: Late Devonian (375–371 Ma)	Exhumation of the sequence, and emplacement by thrust on the top of the Órdenes complex	Broad retrograde metamorphism	Formation of retrograde amphibolites and chlorite-rich schists	Formation of a roughly N–S-trending antiform (arinteiro) during the last Variscan deformation

Macro- and microstructural analyses suggest that the high metamorphic grade and strong deformation developed a foliation in all the rocks, giving rise to S-type mylonites, suggesting a nonhomogeneous pure shear or flattening, which occurred in the Ortegal complex [70]. This flattening and metamorphism prevent us from clearly recognizing the stringer zones of the mineralized areas. Nevertheless, both in the cross-sections (Figure 7) and texturally ("rolled-balls"), in some of these areas, a brecciated feeder zone is detected, inclined at an angle to the rest of the sulfides and showing two preferential directions: N–S-trending (Vieiro) and E–W-trending (Fuente Rosas) (Figures 6–10). A similar situation is presented in [71] for the Palaeoproterozoic Bryah Rift-Basin in Western Australia.

The third step of the evolution of the deposits took place during the Late Devonian (375–371 Ma [72,73]), when the sequence was exhumed and placed by a thrust on the top of the ophiolites of the Órdenes complex. During this process, broad retrometamorphism was developed, and the high-grade metamorphic rocks were transformed into amphibolites and chlorite-rich schists. After this exhumation, a roughly N–S-trending antiform, the Arinteiro (Figure 6), was formed during the last Variscan deformation stage, which is probably related to the Asturian oroclinal development [23–25]. The present contact between the amphibolites, the paragneisses and VMS is tectonic (sheared) due to the contrast of rheological behavior among them. The VMS feeder zones are probably related to the old Ordovician fracture system formed during a rifting process. The copper ore is located in the feeder zones and at the bottom of the basalt laccolith, giving rise to deformed stockworks (breccias) and replacements of the basalts and, on some occasions, the paragneisses.

The metallic mineral paragenesis is mostly composed of pyrrhotite and chalcopyrite, with minor amounts of pyrite and sphalerite. The richest zones in Cu are located at the contact between the stockwork and the replaced basalt. The copper-rich body (>0.2%Cu) is surrounded by a pyrrhotite mass.

As far as the VMS type is concerned, there are three main elements that should be taken into account to classify the deposit. These are mafic volcanics (basalts), massive sulfides within these volcanics and a thick siliciclastic sequence, including the aforementioned volcanics and VMS. Other characteristics to take into account are the predominance of Cu compared to Zn contents and the lack of Pb minerals; the size of over 100 Mt; the amphibolite (basalts) lenses intercalated with metasediments (paragneisses), as is clearly shown in the 3D model; and the absence of felsic rocks. Thus, Touro deposit should be classified as a volcanic massive sulfide (VMS) of the mafic-siliciclastic type [14] that corresponds to the old term "Besshi type" used by [10].

In addition, our geochemical data presented in Figure 5 indicate that the trend of garnet amphibolites, which plot between normal amphibolites and exhalites, may derive

from the metasomatism of basalts by way of the hydrothermal exhalative fluids. In the same way, mineralized brecciated paragneisses are the consequence of the metasomatism of these metasediments by the hydrothermal fluids. Thus, the most likely model for the Touro-mineralized area is the mafic exhalative in a marine siliciclastic sedimentary sequence. As can be seen in the 3D geological model, the host rocks of the deposit are mostly amphibolites with lenticular-shape geometry. They correspond to retrograde-metamorphosed basalts of MORB affinity [60] emplaced in a back-arc basin [58]. The amphibolites are included in paragneisses, which appear to originally have been flysch-type siliciclastic turbidity sediments (Figure 5), including black shales or carbonated rocks.

The main district containing VMS deposits in the Iberian Peninsula is the famous Iberian Pyrite Belt (IPB). As indicated in [15,74], the IPB is located in the South Portuguese Zone and contains the greatest known concentrations of volcanic-hosted massive sulfides (VMS) on Earth. The IPB and Touro districts are both located in the Variscan Iberian Massif, and the mineralizations are VMS, but their characteristics are very different.

The Touro deposit formation is pre-Variscan (Early Ordovician) in a back-arc environment, and the IPB is Variscan and was formed on a stable epicontinental shelf in Devonian–Carboniferous times due to the collision of Laurussia (SPZ) and Gondwana (OMZ and CIZ). Touro is a world-class deposit, with over 100 Mt of ore, but the IPB has also been estimated to hold a minimum resource of more than 1700 Mt of VMS. In Touro, the ore is metamorphosed in amphibolite facies and was highly deformed (flattened); later on, it underwent retrograde metamorphism and was deformed once more. By contrast, the IPB metamorphic grade is mostly very low, typically prehnite-pumpellyite facies, and only in the northern part does it reach the greenschist facies [75]. In addition, deformation is much less intense, and the tectonic structures related to ore formation (extensional faults, pull-aparts, half-graben basins, stringer zones) and host rocks can easily be recognized.

In Touro, it is not easy to recognize the Ordovician stringers, and in the IPB, the basin-forming faults were reactivated as reverse faults with an associated buttressing phenomenon during later Variscan shortening [15].

The igneous rocks at Touro are all mafic and appear to be intruded as laccoliths in the siliciclastic sediments, the ore being directly related to the mafic rocks. In the IPB, the volcanism is bimodal and characterized by andesitic intermediate volcanism, basaltic lava flows, dacitic–rhyolitic dome complexes and sills, interbedded with detrital sedimentary rocks, mostly mudstones with some greywacke and sandstones [74]. The ore can be found both in the sediments and in the felsic volcanism. The abundant bimodal volcanism and the extensive development of VMS mineralization were both mainly emplaced along fracture zones limiting the different basins [74].

Finally, in the Touro deposits, the main ore is Cu with minor Zn and without Pb, whereas in the IPB, Zn and Pb are abundant, and the mineralogy is more complex. Touro can be classified as siliciclastic-mafic, and the IPB as bimodal siliciclastic [74]. Thus, the 3D geological model presented here is an important contribution to the knowledge of the geological evolution of the area.

8. Conclusions

In this work we present, for the first time, a 3D model showing the geometrical characteristics of the world-class VMS Touro deposit. In this 3D geological model, seven main ore bodies were defined, massive sulfides and stringer zones being clearly differentiated in three of them (Fuente Rosas, Vieiro, Arinteiro). In the rest of the bodies, stringer zones (breccia sulfides) are identified, but the drill core data are not sufficient for us to be able to establish a clear relationship between the stringers and VMS.

The 3D model of both the VMS and the amphibolites allowed us to recognize their lenticular-shaped geometry and the relationships between the ores and the host rocks. Most of the sulfides are included in the amphibolites, but on some occasions, they are also in the paragneisses.

The 3D modeling technique, together with the petrographical, mineralogical and some geochemical characteristics of the Touro deposit, has been very useful to define in the Iberian Massif, a siliciclastic-mafic VMS deposit (Besshi type) of over 100 Mt formed in a back-arc environment in rifting. Two preferential directions, N–S and E–W, structurally control the stringer zones identified.

The different amphibolite and paragneiss types show a geochemical trend, indicating that they were affected by hydrothermalism related to ore formation. The amphibolites, originally MORB basalts, become garnet-rich and calcium-poor.

The Touro VMS deposit evolved in three main steps. First, it was formed in an early Ordovician transtensional back-arc environment. Second, it was buried and metamorphosed in amphibolite facies in Early Devonian, and third, it was exhumed and subsequently retrograde-metamorphosed in Late Devonian. As a final conclusion, this 3D geological model provides a better insight to help increase knowledge and facilitates exploration guidelines for this type of VMS deposit in the Órdenes complex.

Supplementary Materials: The following are available online at https://www.mdpi.com/2075-163X/11/1/85/s1, Figure S1: 3D Norte; Figure S2: 3D Fuente Rosas; Figure S3: 3D Touro.

Author Contributions: Conceptualization, M.A., P.G., D.A. and A.M.-I.; methodology, M.A., P.G., D.A. and P.N.; software, M.A., P.G. and C.C.; validation, M.A., A.M.-I., D.A., P.G. and P.N.; investigation, P.N., J.F.-B., M.A., D.A., P.G. and A.M.-I.; resources, P.N. and C.C.; data curation, D.A., M.A. and P.G.; writing—original draft preparation, M.A., P.G., P.N. and J.F.-B.; writing—review and editing A.M.-I. and D.A.; visualization, M.A. and P.N.; supervision, A.M.-I., P.G. and M.A.; project administration, A.M-I. and D.A.; funding acquisition, A.M.-I., D.A., M.A. and P.N. All authors have read and agreed to the published version of the manuscript.

Funding: This research was funded by Ministerio de Economía, Industria y Competitividad, Gobierno de España, project CGL2016-76532R (AEI/FEDER/UE).

Institutional Review Board Statement: Not applicable.

Informed Consent Statement: Not applicable.

Data Availability Statement: Data is contained within the article or supplementary material.

Acknowledgments: The authors would like to thank the Atalaya Mining and Cobre San Rafael companies for access to the drilling cores, logs and other data provided. We also thank John Hardwick for his help in reviewing the English of the paper. We want also to thank the old staff of the Lundin Department of Geology for their drill core logs, geochemical analyses and contribution to the knowledge of this area of world relevance. We are grateful to three anonymous reviewers for their comments and suggestions that greatly increase the clarity and quality of the paper.

Conflicts of Interest: The authors declare no conflict of interest.

References

1. Farias, P.; Gallastegui, G.; Lodeiro, F.G.; Marquínez, J.; Parra, L.M.M.; De Pablo Macía, J.G.; Fernández, L.R.R. Aportaciones al conocimiento de la litoestratigrafia y estructura de Galicia Central. *Mem. Fac. Ciências Univ. Porto* **1987**, *1*, 411–431.
2. Julivert, M.; Fontboté, J.M.; Ribeiro, A.; Conde, L.E.N. *Mapa Tectónico de la Península Ibérica y Baleares, E 1:1000000, Memoria Explicativa*; Instituto Geológico y Minero de España: Madrid, Spain, 1972; p. 113.
3. Pérez-Estaún, A.; Bastida, F.; Catalán, J.R.M.; Marco, J.C.G.; Marcos, A.; Pulgar, J.A. West Asturian–Leonese zone, stratigraphy. In *Pre-Mesozoic Geology of Iberia*; Dallmeyer, R.D., Martínez-García, E., Eds.; Springer: Berlin/Heidelberg, Germany, 1990; pp. 92–102.
4. Castiñeiras, P. Origen y Evolución Tectonotermal de las Unidades de O Pino y Cariño (Complejos Alóctonos de Galicia). Ph.D. Thesis, Universidad Complutense de Madrid, Madrid, Spain, 2005; p. 289, Serie Terra Nova 28.
5. Arenas, R.; Martínez, S.S.; Díez Fernández, R.; Gerdes, A.; Abati, J.; Fernández-Suárez, J.; Andonaegui, P.; Cuadra, P.G.; Carmona, A.L.; Albert, R.; et al. Allochthonous terranes involved in the Variscan suture of NW Iberia: A review of their origin and tectonothermal evolution. *Earth Sci. Rev.* **2016**, *161*, 140–178. [CrossRef]
6. Barreiro, J.G.; Catalán, J.R.M.; Fernández, R.D.; Arenas, R.; García, F.D. Upper crust reworking during gravitational collapse: The Bembibre-Pico Sacro detachment system (NW Iberia). *J. Geol. Soc.* **2010**, *167*, 769–784. [CrossRef]
7. Díez Fernández, R.; Catalán, J.R.M.; Martín, R.A.; Gómez, J.A. Tectonic evolution of a continental subduction-exhumation channel: Variscan structure of the basal allochthonous units in NW Spain. *Tectonics* **2011**, *30*, TC3009. [CrossRef]

8. Julivert, M.; Martínez, F.J. The Structure and Evolution of the Hercynian Fold Belt in the Iberian Peninsula. In *The Anatomy of Mountain Ranges, Princeton Legacy Library and Princeton Series in Geology and Paleontology, 788*; Schaer, J.-P., Rodgers, J., Eds.; Princeton University Press: Princeton, NJ, USA, 2014; Chapter 6; pp. 65–105.
9. Catalán, J.R.M.; Lobato, F.Á.; Pinto, V.; Barreiro, J.G.; Ayarza, P.; Villalaín, J.J.; Casas, A. Gravity and magnetic anomalies in the allochthonous Órdenes Complex (Variscan belt, northwest Spain): Assessing its internal structure and thickness Tectonics. *J. Geol.* **2012**, *31*, TC5007.
10. Badham, P.; Williams, J. Genetic and Exploration Models for Sulfide Ores in Metaophiolites, Northwest Spain. *Econ. Geol.* **1981**, *76*, 2118–2127. [CrossRef]
11. Sides, E.J. An alternative approach to the modelling of deformed stratiform and stratabound deposits. In Proceedings of the Twentieth lnternational Symposium on the Application of computers and Mathematics in the Mineral Industries, Johannesburg, South Africa, 19–23 October 1987; Volume 3, pp. 187–198.
12. Serranti, S.; Ferrini, V.; Masi, U.; Nicoletti, M.; Conde, L. Geochemical features of the massive sulfide (Cu) metamorphosed deposit of Arinteiro (Galicia, Spain) and genetic implications. *Period. Mineral.* **2002**, *71*, 27–48.
13. Williams, P.J. The genesis and metamorphism of the Arinteiro-Bama Cu deposits, Santiago de Compostela, northwestern Spain. *Econ. Geol.* **1983**, *78*, 1689–1700. [CrossRef]
14. Galley, A.G.; Hannington, M.D.; Jonasson, I.R. Volcanogenic massive sulphide deposits. *Geol. Assoc. Can. Miner. Depos. Div. Spec. Publ.* **2007**, *5*, 141–161.
15. Martin-Izard, A.; Arias, D.; Arias, M.; Gumiel, P.; Sanderson, D.J.; Castañón, C.; Lavandeira, A.; Sanchez, J. A new 3D geological model and interpretation of structural evolution of the world-class Rio Tinto VMS deposit, Iberian Pyrite Belt (Spain). *Ore Geol. Rev.* **2015**, *71*, 457–476. [CrossRef]
16. Kampmann, T.C.; Stephens, M.B.; Weihed, P. 3D modelling and sheath folding at the Falun pyritic Zn-Pb-Cu-(Au-Ag) sulphide deposit and implications for exploration in a 1.9 Ga ore district, Fennoscandian Shield, Sweden. *Miner. Depos.* **2016**, *51*, 665–680. [CrossRef]
17. Schetselaar, E.; Pehrsson, S.; Devine, C.; Lafrance, B.; White, D.; Malinowski, M. 3-D geologic modeling in the Flin Flon mining district, Trans-Hudson orogen, Canada: Evidence for polyphase imbrication of the Flin Flon-777-Callinan volcanogenic massive sulfide ore system. *Econ. Geol.* **2016**, *111*, 877–901. [CrossRef]
18. López-Burgos, M.A. La mineria española en la obra impressions of Spain de Albert, F. Calvert. *Cuad. Geográficos* **2005**, *37*, 227–270.
19. Calvert, A. *Impressions of Spain*; London, P., Ed.; University of California Libraries: Oakland, CA, USA, 1903; p. 363.
20. Technical Report On the Mineral Resources and Reserves of the Touro Copper Project. Available online: https://atalayamining.com/wp-content/uploads/2020/01/NI-43-101-Technical-Report-for-Proyecto-Touro.pdf (accessed on 7 January 2021).
21. Díez-Fernández, R.; Arenas, R.; Francisco-Pereira, M.; Sánchez-Martínez, S.; Albert, R.; Martín Parra, L.M.; Rubio Pascual, F.J.; Matas, J. Tectonic evolution of Variscan Iberia: Gondwana–Laurussia collision revisited. *Earth Sci. Rev.* **2016**, *162*, 269–292. [CrossRef]
22. Matte, O. The Variscan collage and orogeny (480 ± 290 Ma) and the tectonic definition of the Armorica microplate: A review. *Terra Nova* **2001**, *13*, 122–128. [CrossRef]
23. Alonso, J.L.; Marcos, A.; Suárez, A. Paleogeographic inversion resulting from large out of sequence breaching thrusts: The León Fault (Cantabrian Zone, NW Iberia). A new picture of the external Variscan Thrust Belt in the Ibero-Armorican Arc. *Geol. Acta* **2009**, *7*, 451–473.
24. Gutiérrez-Alonso, G.; Collins, A.S.; Fernández-Suárez, J.; Pastor-Galán, D.; González-Clavijo, E.; Jourdan, F.; Weil, A.B.; Johnston, S.T. Dating of lithospheric buckling: 40Ar/39Ar ages of syn-orocline strike–slip shear zones in northwestern Iberia. *Tectonophysics* **2015**, *643*, 44–54. [CrossRef]
25. Pastor-Galán, D.; Gutiérrez-Alonso, G.; Murphy, J.B.; Fernández-Suárez, J.; Hofmann, M.; Linnemann, U. Provenance analysis of the Paleozoic sequences of the northern Gondwana margin in NW Iberia: Passive margin to Variscan collision and orocline development. *Gondwana Res.* **2013**, *23*, 1089–1103. [CrossRef]
26. Catalán, R.M.; Arenas, R.; García, F.D.; Abati, J. Variscan accretionary complex of northwest Iberia: Terrane correlation succession of tectonothermal events. *Geology* **1997**, *25*, 1103–1106. [CrossRef]
27. Noblet, C.; Lefort, J.P. Sedimentological evidence for a limited separation between Armorica and Gondwana during the Early Ordovician. *Geology* **1990**, *18*, 303–306. [CrossRef]
28. Ziegler, P.A. (Ed.) Hercynian Suturing of Pangea. In *AAPG Memoir Vol. 43: Evolution of the Arctic-North Atlantic and the Western Tethys*; The American Association of Petroleum Geologists: Tulsa, OK, USA, 1988; pp. 25–32.
29. Díez Fernández, R.; Catalán, J.R.M.; Arenas, R.; Abati, J.; Gerdes, A.; Fernández-Suárez, J. U–Pb detrital zircon analysis of the lower allochthon of NW Iberia: Age constraints, provenance and links with the Variscan mobile belt and Gondwanan cratons. *J. Geol. Soc.* **2012**, *169*, 655–665. [CrossRef]
30. Catalán, J.R.M.; Arenas, R.; Abati, J.; Martínez, S.S.; García, F.D.; Suárez, J.F.; Cuadra, P.G.; Castiñeiras, P.; Barreiro, J.G.; Montes, A.D.; et al. A rootless suture and the loss of the roots of a mountain chain: The Variscan belt of NW Iberia. *Comptes Rendus Geosci.* **2009**, *341*, 114–126.
31. Scotese, C.R.; Boucot, A.J.; Mckerrow, W.S. Gondwanan palæogeography and palæoclimatology. *J. Afr. Earth Sci.* **1999**, *28*, 99–114. [CrossRef]

32. Arenas, R.; Sánchez Martínez, S.; Gerdes, A.; Albert, R.; Díez Fernández, R.; Andonaegui, P. Re-interpreting the Devonian ophiolites involved in the Variscan suture: U-Pb and Lu-Hf zircon data of the Moeche Ophiolite (Cabo Ortegal Complex, NW Iberia). *Int. J. Earth Sci.* **2014**, *103*, 1385–1402. [CrossRef]
33. Van Zuuren, A. Structural petrology of an area near Santiago de Compostela (NW Spain). *Leidse Geol. Meded.* **1970**, *45*, 1–71.
34. Catalán, J.M.; García, F.D.; Arenas, R.; Abati, J.; Castiñeiras, P.; Cuadra, P.G.; Barreiro, J.G.; Pascual, F.J.R. Thrust and detachment systems in the Ordenes Complex (northwestern Spain) implications for the Variscan-Appalachian geodynamics. In *Variscan-Appalachian Dynamics: The Building of the Late Paleozoic Besement*; Catalán, J.R.M., Hatcher, R.D., Jr., Arenas, R., Garcia, F.D., Eds.; Geological Society of America: Boulder, CO, USA, 2002; Volume 364, pp. 163–182.
35. Castroviejo, R.; Armstrong, E.; Lago, A.; Simón, J.M.M.; Argüelles, A. Geología de las mineralizaciones de sulfuros masivos en los cloritoesquistos de Moeche (complejo de Cabo Ortegal, A Coruña). *Bol. Geol. Min.* **2004**, *115*, 3–34.
36. Abati, J. *Petrología Metamórfica y Geocronología de la Unidad Culminante del Complejo de Órdenes en la Región de Carballo (Galicia, NW del Macizo Ibérico)*; Sada, A., Ed.; Ediciós do Castro: La Coruña, Spain, 2002; p. 269.
37. Barreiro, J.G.; Catalán, J.R.M.; Arenas, R.; Castiñeiras, P.; Abati, J.; García, F.D.; Wijbrans, J.R. *The Evolution of the Rheic Ocean: From Avalonian-Cadomian Active Margin to Alleghenian-Variscan Collision*; Geological Society of America: Boulder, CO, USA, 2007; Volume 423.
38. Arenas, R.; Farias, P.; Gallastegui, G.; Gil Ibarguchi, J.I.; Lodeiro, F.G.; Klein, E.; Marquínez, J.; Parra, L.M.M.; Catalán, J.R.M.; Ortega, E.; et al. Características geológicas y significado de los dominios que componen la Zona de Galicia-Trás-os-Montes. In Simposio Sobre Cinturones Orogénicos. In Proceedings of the II Congreso Geológico de España, Granada, Spain, 14–18 July 1988; pp. 75–84.
39. Martínez Catalán, J.R.; Arenas, R.; Abatí, J.; Martínez, S.; García, F.; Fernández-Suárez, J.; Cuadra, P.; Castiñeiras, P.; Gómez Barreiro, J.; Díez-Montes, A.; et al. *Geología del Complejo de Cabo Ortegal y de las Unidades Relacionadas del Basamento de Galicia*; Concello de Cariño: Cariño, Spain, 2010; p. 133.
40. Gil Ibarguchi, J.I.; Ábalos, B.; Puelles, P.A. Deformation, high-pressure metamorphism and exhumation of ultramafic rocks in a deep subduction/collision setting (Cabo Ortegal, NW Spain). *J. Metamorph. Geol.* **1999**, *17*, 747–764. [CrossRef]
41. Marcos, A.; Marquínez, J.; Perez-Estaún, A.; Pulgar, J.; Bastida, F. Nuevas aportaciones al conocimiento de la evolución tectonometamórfica del complejo de Cabo Ortegal (NW de España). *Cuadernos Laboratorio Xeolóxico Laxe* **1984**, *7*, 125–137.
42. Gómez Barreiro, J.; Catalán, J.R.; Arenas, R.; Castiñeiras, P.; Abati, J.; García, F.; Wijbrans, J.R.; Barreiro, G.; Catalán, M.; Castiñeiras, R.; et al. Tectonic Evolution of the Upper Allochthon of the Órdenes Complex (Northwestern Iberian Massif): Structural Constraints to a Polyorogenic Peri-Gondwanan Terrane. In *The Evolution of the Rheic Ocean: From Avalonian-Cadomian Active Margin to Alleghenian-Variscan Collision*; Geological Society of America: Boulder, CO, USA, 2007.
43. Arenas, R.; Catalán, J.R.M. Prograde Development of Corona Textures in Metagabbros of the Sobrado Unit (Ordenes Complex, Northwestern Iberian Massif). *Spec. Pap. Geol. Soc. Am.* **2002**, *364*, 73–88.
44. Gil Ibarguchi, J.I.; Arenas, R. Metamorphic evolution of the allochthonous complexes from the northwest of Iberian Peninsula. In *Pre-Mesozoic Geology of Iberia*; Dallmeyer, R.D., Martínez-García, E., Eds.; Springer: Berlin/Heidelberg, Germany, 1990; pp. 237–246.
45. Aranguren, M.S.M.; Gil Ibarguchi, J.I. Petrología de la Unidad Eclogítica del Complejo de Cabo Ortegal (NW de España). Ph.D. Thesis, Universidad Del Pais Vasco, Biscay, Spain, 2000; p. 425, Terra Nova 16.
46. Vogel, D.E. Petrology of an eclogite- and pyrigarnite-bearing polymetamorphic rock complex at Cabo Ortegal, NW Spain. *Leidse Geol. Meded.* **1967**, *40*, 121–213.
47. Catalán, J.M.; Martín, R.A. Deformación extensional de las unidades alóctonas superiores de la parte oriental del Complejo de Ordenes (Galicia). *Geogaceta* **1992**, *11*, 108–111.
48. Rodríguez-Terente, L.M.; Martin-Izard, A.; Arias, D.; Fuertes-Fuente, M.; Cepedal, A. The Salave Mine, a Variscan intrusion-related gold deposit (IRGD) in the NW of Spain: Geological context, hydrothermal alterations and ore features. *J. Geochem. Explor.* **2018**, *188*, 364–389. [CrossRef]
49. Houlding, S.W. *3D Geoscience Modeling-Computer Techniques for Geological Characterization*; Springer: Berlin/Heidelberg, Germany, 1994; pp. 1–6.
50. Lemon, A.M.; Jones, N.L. Building solid models from boreholes and user- defined cross-sections. *Comput. Geosci.* **2003**, *29*, 547–555. [CrossRef]
51. Calcagno, P.; Courrioux, G.; Guillen, A.; Chiles, J.P. Geological modelling from field data and geological knowledge. Part I. modelling method coupling 3D potential field interpolation and geological rules. *Phys. Earth Planet. Inter.* **2008**, *171*, 147–157. [CrossRef]
52. Kaufmann, O.; Martin, T. 3D geological modelling from boreholes, cross-sections and geological maps, application over former natural gas storages in coal mines. *Comput. Geosci.* **2008**, *34*, 278–290, reprint in *Comput. Geosci.* **2009**, *35*, 70–82. [CrossRef]
53. Maxelon, M.; Renard, P.; Courrioux, G.; Brandli, M.; Mancktelow, N. A workflow to facilitate three-dimensional geometrical modelling of complex poly-deformed geological units. *Comput. Geosci.* **2009**, *35*, 644–658. [CrossRef]
54. Schetselaar, E.; Ames, D.; Grunsky, E. Integrated 3D Geological Modeling to Gain Insight in the Effects of Hydrothermal Alteration on Post-Ore Deformation Style and Strain Localization in the Flin Flon Volcanogenic Massive Sulfide Ore System. *Minerals* **2018**, *8*, 3. [CrossRef]

55. Lajaunie, C.; Courrioux, G.; Manuel, L. Foliation fields and 3D cartography in geology: Principles of a method based on potential interpolation. *Math. Geol.* **1997**, *29*, 571–584. [CrossRef]
56. Gumiel, P.; Arias, M.; Martín-Izard, A. 3D geological modelling of a polyphase deformed pre-Variscan IOCG mineralization located at the southeastern border of the Ossa Morena Zone, Iberian Massif (Spain). *Geol. J.* **2010**, *45*, 623–633. [CrossRef]
57. McKinstry, H.E. *Geología De Minas*; Omega: Barcelona, Spain, 1970; p. 671.
58. Marjoribanks, R. *Geological Methods in Mineral Exploration and Mining*; Springer: Berlin, Germany, 2010; p. 233.
59. Heiman, A.; Spry, P.G.; Teale, G.S.; Conor, C.H.; Leyh, W.R. Geochemistry of Garnet-Rich Rocks in the Southern Curnamona Province, Australia, and Their Genetic Relationship to Broken Hill-Type Pb-Zn-Ag Mineralization. *Econ. Geol.* **2009**, *104*, 687–712. [CrossRef]
60. Calcagno, P.; Martelet, G.; Gumiaux, C. Apport de la modélisation géométrique 3D a'l'interprétation géologique du complexe de Champtoceaux (massif armoricain). In Proceedings of the 19e'me RST Congress, Nantes, France, 9–12 April 2002; p. 79.
61. Boissonnat, J.D. Shape reconstruction from planar cross-sections. *Comput. Vis. Graph. Image Process.* **1988**, *44*, 1–29. [CrossRef]
62. Bertrand, P.; Dufour, J.F.; Francon, J.; Lienhardt, P. *Modélisation Volumique à base Topologique*; Actes MICAD: Hermès, Paris, 1992; Volume 1, pp. 59–74.
63. Böstrom, K. The origin and fate of ferro-mangano in active ridge sediments. *Stockh. Contrib. Geol.* **1973**, *27*, 147–243.
64. Spry, P.G.; Peter, J.M.; Slack, J.F. *Meta-Exhalites as Exploation Guides to Ore: Reviews in Economic Geology*; Society of Economic Geologists: Lyttelton, CO, USA, 1998; Volume 11, pp. 163–201.
65. Peter, J.M.; Goodfellow, W.D.; Doherty, W. Hydrothermal Sedimentary Rocks of the Heath Steele Belt, Bathurst Mining Camp, New Brunswick: Part 2. Bulk and Rare Earth Element Geochemistry and Implications for Origin. *Econ. Geol. Monogr.* **2003**, *11*, 391–415.
66. Santos Zalduegui, J.F.; Scharer, U.; Gil Ibarguchi, J.I.; Girardeau, J. Origin and evolution of the Paleozoic Cabo Ortegal ultramafic-mafic complex (NW Spain): U-Pb, Rb-Sr and Pb-Pb isotope data. *Chem. Geol.* **1996**, *129*, 281–304. [CrossRef]
67. Ordóñez Casado, B.; Gebauer, D.; Schafer, H.J.; Gil Ibarguchi, J.I.; Peucat, J.J. A single Devonian subduction event for the HP/HT metamorphism of the Cabo Ortegal complex within the Iberian Massif. *Tectonophysics* **2001**, *332*, 359–385.
68. Fernández-Suárez, J.; Corfu, F.; Arenas, R.; Marcos, A.; Martínez Catalán, J.R.; Díaz García, F.; Abati, J.; Fernández, F.J. U-Pb evidence for a polyorogenic evolution of the HPHT units of the NW Iberian Massif. Contrib. *Miner. Petrol.* **2002**, *143*, 236–253.
69. Fernández-Suárez, J.; Arenas, R.; Abati, J.; Martínez Catalán, J.R.; Whitehouse, M.J.; Jeffries, T.E. U-Pb chronometry of polymetamorphic high-pressure granulites: An example from the allochthonous terranes of the NW Iberian Variscan belt. *Geol. Soc. Am. Mem.* **2007**, *200*, 469–488.
70. Fernandez, F.J.; Marcos, A. Mylonitic foliation developed by heterogeneous pure shear under high-grade conditions in quartz feldspathic rocks (Chimparra gneiss formation, Cabo Ortegal complex, NW Spain). In *Basement Tectonics 11 Europe and Other Regions*; Springer: Berlin, Germany, 1996; pp. 17–34.
71. Pirajno, F.; Chen, Y.; Li, N.; Li, C.; Zhou., L.D. Besshi-type mineral systems in the Palaeoproterozoic Bryah Rift-Basin, Capricorn Orogen, Western Australia: Implications for tectonic setting and geodynamic evolution. *Geosci. Front.* **2016**, *7*, 345–357. [CrossRef]
72. Dallmeyer, R.D.; Martínez Catalán, J.R.; Arenas, R.; Gil Ibarguchi, J.I.; Gutiérrez-Alonso, G.; Farias, P.; Bastida, F.; Aller, J. Diachronous Variscan tectonothermal activity in the NW Iberian Massif: Evidence from 40Ar/39Ar dating of regional fabrics. *Tectonophysics* **1997**, *277*, 307–337. [CrossRef]
73. Gómez Barreiro, J.; Wijbrans, J.R.; Castineiras, P.; Martínez Catalán, J.R.; Arenas, R.; Díaz García, F.; Abati, J. 40Ar/39Ar laser probe dating of mylonitic fabrics in a polyorogenic terrane of NW Iberia. *J. Geol. Soc.* **2006**, *163*, 61–73.
74. Martin-Izard, A.; Arias, D.; Arias, M.; Gumiel, P.; Sanderson, D.J.; Castañon, C.; Sanchez, J. Ore deposit types and tectonic evolution of the Iberian Pyrite Belt: From transtensional basins and magmatism to transpression and inversion tectonics. *Ore Geol. Rev.* **2016**, *79*, 254–267. [CrossRef]
75. Munhá, J. Metamorphic evolution of the South Portuguese/Pulo do Lobo Zone. In *Pre-Mesozoic Geology of Iberia*; Dallmeyer, R.D., Martínez García, E., Eds.; Springer: Berlin/Heidelberg, Germany, 1990; pp. 363–368.